Hindawi
International Journal of RF and Microwave Computer-Aided Engineering
Volume 2024, Article ID 6618418, 8 pages
https://doi.org/10.1155/2024/6618418

Research Article

A Simultaneously Transmit and Receive Antenna Terminal for In-Band Full-Duplex Applications

Meenal [1,2] **and Amalendu Patnaik** [1]

[1]*Department of Electronics and Communication Engineering, Indian Institute of Technology Roorkee, Roorkee, Uttarakhand, India*
[2]*Semi-Conductor Laboratory, Ministry of Electronics and Information Technology, S.A.S Nagar, Punjab, India*

Correspondence should be addressed to Amalendu Patnaik; amalendu.patnaik@ece.iitr.ac.in

Received 23 December 2023; Revised 21 February 2024; Accepted 1 March 2024; Published 25 March 2024

Academic Editor: N. Nasimuddin

In this paper, a low-profile co-linearly polarized simultaneously transmit-receive antenna (STRA) terminal is presented for 5G and upcoming technologies. The proposed STRA terminal comprises of an identical pair of spatially rotated half-circular microstrip antennas for transmission (Tx) and reception (Rx). The challenge of self-interference (SI) is addressed by employing passive SI cancellation techniques such as spatial diversity, field confinement, and surface perturbations. This has been accomplished by using fence-strip structure and V-shaped slots in the ground plane. The STRA was designed, fabricated, and tested for full-duplex operation in a sub-6 GHz band lying from 5.73 to 5.88 GHz, providing high interport isolation ranging from 35.5 dB to a maximum of 46.5 dB. The proposed STRA was implemented using Rogers 3003™ substrate. The measurements yield radiation characteristics with high gain of 5.45-6.0 dBi and 5-6.5 dBi for Tx and Rx antennas, respectively. The measured results are in good conformance with the simulated design. This antenna finds its potential usage in V2X and private 5G networks and can be extended for full-duplex MIMO implementations.

1. Introduction

With an exponential rise in wireless applications and considering the limited availability of frequency spectrum, the need for systems with high data rates and throughput is inevitable. The fifth generation (5G) wireless systems have catered these needs for high efficiency, high data rates, and better connectivity. However, wireless communication systems conventionally operate in half-duplex mode which results in underutilization of the available bandwidth. In recent years, in-band full-duplex systems have gained significant attention as they can simultaneously transmit and receive within the same frequency bands and hence, technically, may double the spectral efficiency. For the successful implementation of full-duplex communication, interference cancellations at multiple stages in the transmit and receive chain are required. This is accomplished at various subsystems working in the digital domain, analog domain, and propagation domain [1, 2]. In addition, a careful design of transmit and receive terminals with high interport isolation further aids the cancellation process in the subsequent stages. Recently, many techniques have been reported to improve interport isolation at antenna terminals in the propagation domain.

In [3], a full-duplex antenna has been presented for 5G applications operating in a frequency band of 2.40-2.62 GHz with an isolation ranging from 35.9 to 46.5 dB. In this scheme, a reflective terminal is used to cancel the direct coupling between the transmit and receive antenna. Whereas by employing differential feeding schemes and/or 180° hybrid couplers for patch antenna, interport isolation ranging from 40 to 90 dB can be achieved [4–8]. However, it can be observed that high levels of isolation are achieved at the cost of bandwidth. Another approach using orthogonal spatial phase diversity has been demonstrated to provide isolation better than 37 dB across the band of 2.3-2.9 GHz in [9]. This antenna consists of a turnstile antenna as the transmitter (Tx) and a loop antenna as the receiver (Rx) stacked vertically. In [10], a gear-shaped monostatic antenna is used for Tx and Rx. Here, the incorporation of a defected ground structure

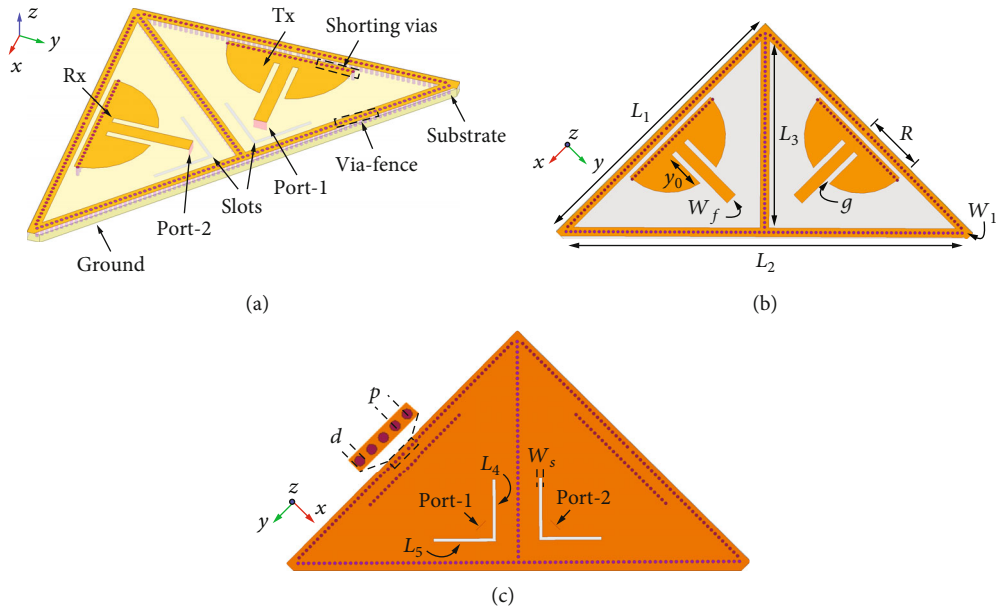

FIGURE 1: Geometry of the proposed antenna. (a) Isometric view, (b) top view, and (c) bottom view. Dimensions: $L_1 = 50$; $R = 9.6$; $L_2 = 68.5$; $W_1 = 1.5$; $L_3 = 31.5$; $W_s = 0.5$; $l_s = 9.5$; $W_f = 2$; $w_s = 0.5$; $y_0 = 6.8$; $d = 0.5$; $g = 0.9$; $p = 0.8$; $h = 1.52$. Units in mm.

offers frequency filtering and results in isolation between Tx and Rx terminals. An even and odd mode feed-based approach has been mentioned in [11] for in-band full-duplex applications. In [12], a broadband, differentially fed patch antenna based on metasurface, has been demonstrated to exhibit isolation better than 43 dB. Another full-duplex antenna using a fence-strip resonator has been reported in [13]. This antenna offers isolation better than 20 dB over an operating bandwidth of 2.4-2.52 GHz.

In this work, we present a low-profile, in-band full-duplex simultaneously transmit-receive antenna (STRA) operating over a bandwidth of 150 MHz from 5.73 to 5.88 GHz for 5G and upcoming technologies. The antenna offers isolation as high as 46.5 dB between the Tx and Rx antennas by utilizing a combination of spatial diversity, field confinement, and surface current cancellations.

2. Antenna Realization

2.1. Configuration of Proposed Antenna. The proposed antenna consists of a pair of half-circular microstrip antennas colocated spatially with orthogonal placement as shown in Figure 1. The half-circular configuration is implemented by loading an array of via holes along the center normal to the E-plane. Both antennas are inset-fed by microstrip lines and are identical in nature. A series of vias forming a fence structure is incorporated along the periphery of these radiators for field confinement. Furthermore, a compact V-shaped slot is incorporated near the feed point of each radiator in the ground plane. These measures reduce coupling between the adjacent feed ports and result in high interport isolation.

2.2. Evolution of Proposed Antenna. Initially, a pair of half-circular microstrip antennas located orthogonally is designed to operate at 5.8 GHz (design-1 in Figure 2). However, it can be seen from the S-parameter plot that mere orthogonal placement is not sufficient as strong coupling occurs between the two ports yielding isolation of 27 dB. To address this issue, in the next step, a via fence is introduced along the periphery which acts as a vertical electric wall and thus enables field confinement (design-2 in Figure 2). This improves isolation by 5 dB, and thus, interport isolation better than 32 dB is achieved. Finally, V-shaped slots are introduced in the ground plane near the feed point of each radiator (design-3 in Figure 2). The slot modifies the surface current in the ground plane as it acts as an inductive element and results in additional resonance (surface current density distributions in Figure 2)). This additional parallel resonance possesses band-stop characteristics resulting in isolation enhancement up to 45 dB at 5.8 GHz. In addition, the radiation patterns are also not altered in the direction of maximum radiation, and the front-to-back ratio is 9.7 dB which is within the acceptable limits for wireless communications (Figure 2).

2.3. Design of Proposed Antenna. For the implementation of the proposed STRA, initially, a circular microstrip antenna inset-fed by a microstrip line was designed. This antenna operates at dominant TM_{110} mode, and the dimensions were determined as follows [14]:

$$f_r = \frac{1}{2\pi\sqrt{\mu\epsilon}}\frac{\chi'_{11}}{R}, \tag{1}$$

where χ'_{11} represents the first zero of the Bessel function for TM_{110} mode and R is the radius of the microstrip patch. Next, the half-circular configuration was implemented by loading an array of via holes along the center normal to

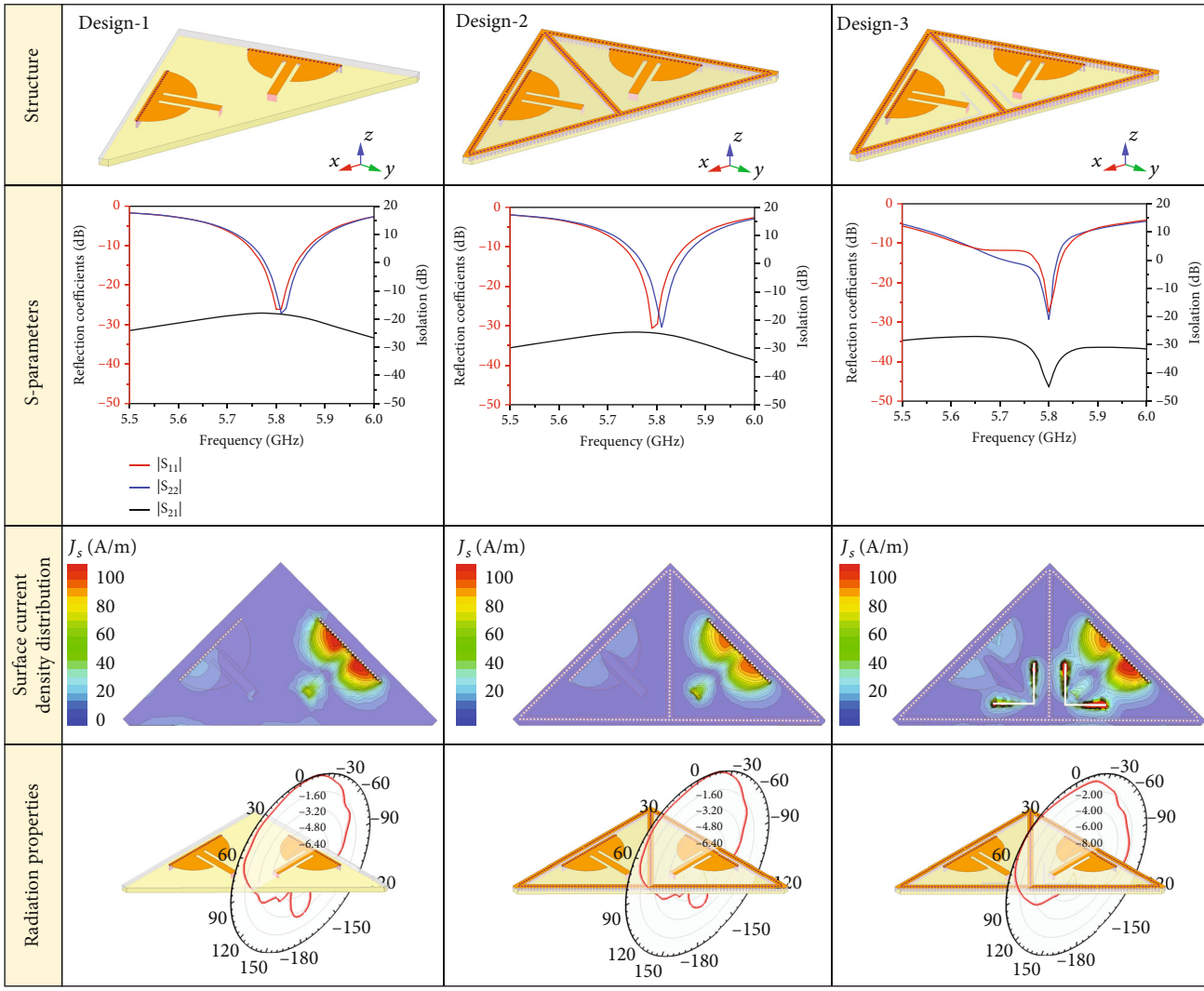

Figure 2: Design evolution of the proposed antenna. Comparison in terms of S-parameters, surface current density distributions, and radiation properties.

the E-plane. The pitch, p, and diameter, d, of the designed via holes satisfy the following:

$$\lambda_g = \frac{\lambda_0}{\sqrt{\epsilon_r}},$$
$$d \leq \frac{\lambda_g}{5}, \tag{2}$$
$$p \leq 2d,$$

where λ_g is the guided wavelength and λ_0 is the free space wavelength at the center frequency. After that, two of these antennas were positioned orthogonally, and a fence-strip structure was implemented along the perimeter with pitch, p, and diameter, d, satisfying equation (2). Next, a pair of V-slots for the ground plane was designed to operate at 5.8 GHz. As the slot interior angle increases, the rejection bandwidth also increases. However, given the constraints of space, the interior angle of the V-slot was chosen to be 90°. For the band-stop characteristics, the dimensions were optimized by running a parametric analysis as shown in Figure 3. From the parametric study, it can be observed that with the increase in slot length, l_s, the stop-band shifts to lower frequency values.

The final dimensions of each element were optimized by carrying out parametric analysis in Ansys High-Frequency Structure Simulator v2021R3.

3. Results and Discussion

The proposed antenna was designed and fabricated using a 1.52 mm thick Rogers RO3003™ substrate with a relative permittivity of 3.0 and dielectric loss tangent of 0.0001. The prototype was fabricated in-house by a standard photolithographic procedure for printed circuits.

Next, the experimental validation of the proposed STRA was carried out by measuring S-parameters and radiation profiles. The S-parameter measurements were carried out

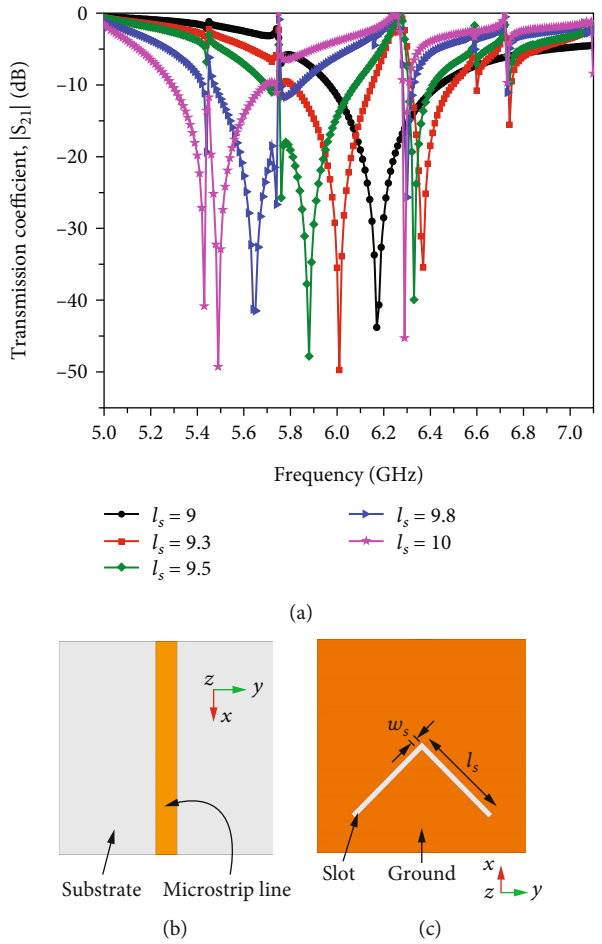

FIGURE 3: (a) Parametric study of slot length. (b) Top view: microstrip line. (c) Bottom view: slot embedded in the ground.

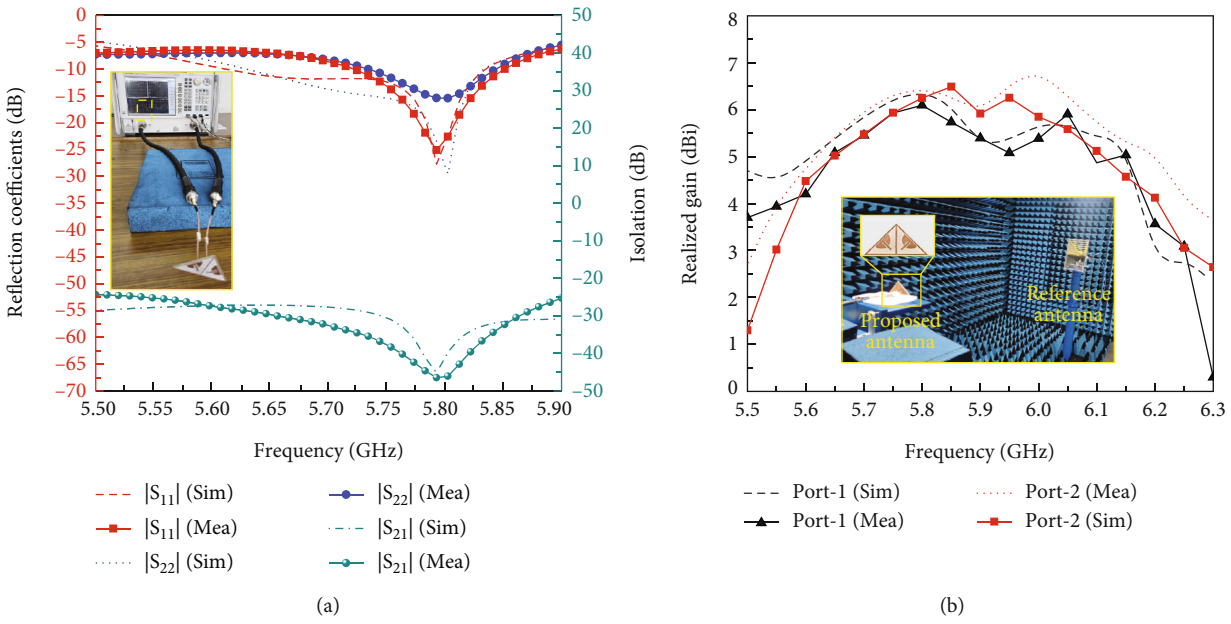

FIGURE 4: Simulated and measured results for port-1 and port-2. (a) S-parameter results with measurement setup and (b) realized gain results with measurement setup in anechoic chamber.

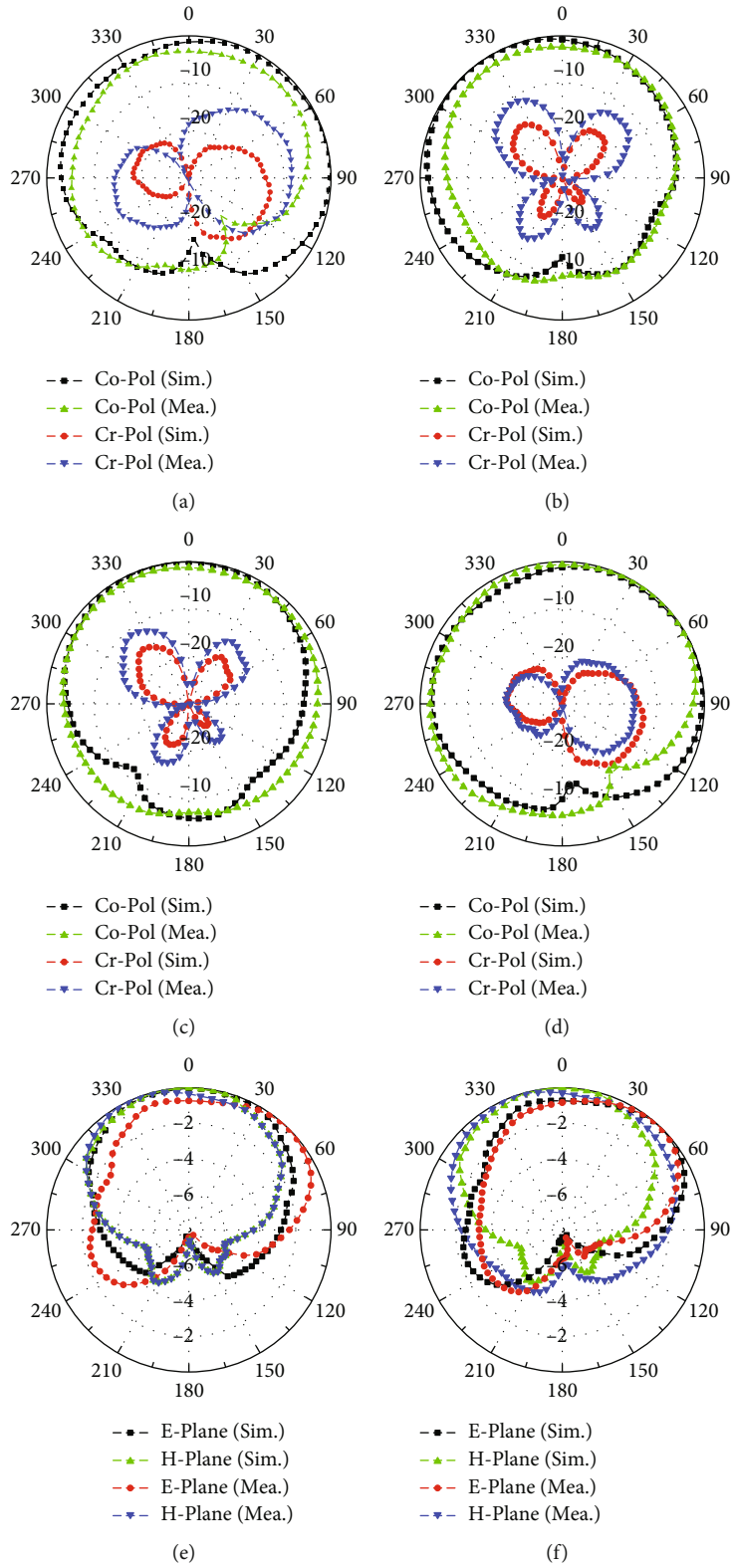

Figure 5: Simulated and measured radiation characteristics of port-1 and port-2. (a) Co. and cross polarizations in the E-plane of port-1. (b) Co. and cross polarizations in the H-plane of port-1. (c) Co. and cross polarizations in the E-plane of port-2. (d) Co. and cross polarizations in the H-plane of port-2. (e) Radiation pattern for port-1. (f) Radiation pattern for port-2.

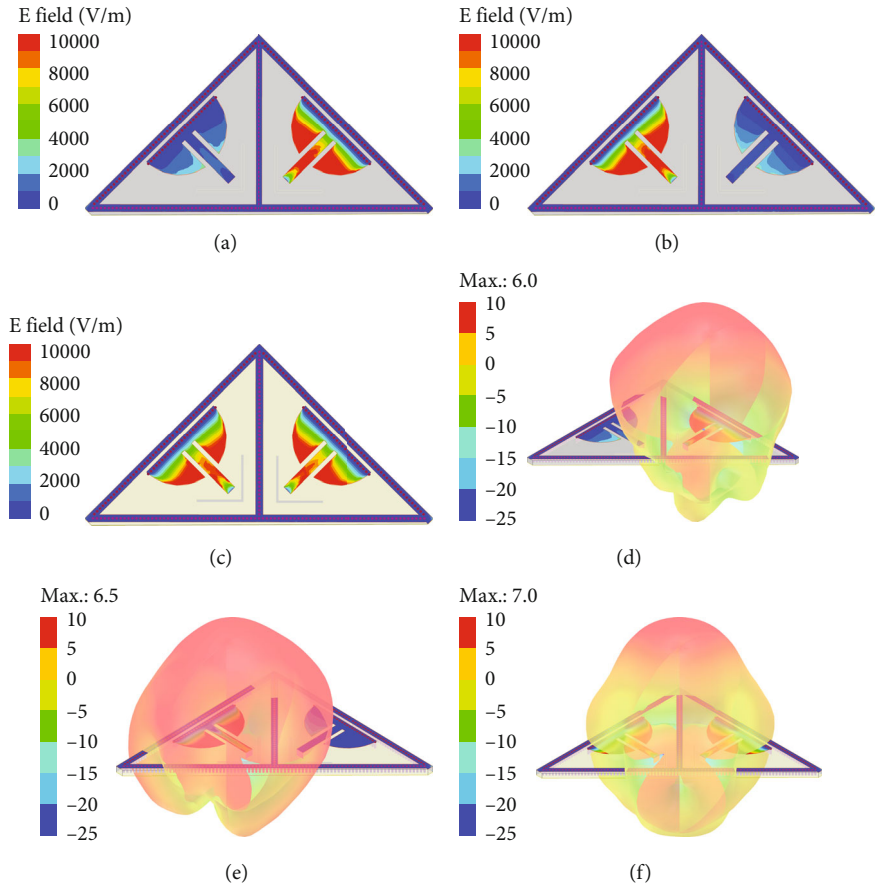

FIGURE 6: (a) E-field at port-1, port-2 terminated with matched load. (b) E-field at port-2, port-1 terminated with matched load. (c) E-field at port-1, port-2 with simultaneous excitation. (d) Gain at port-1, port-2 terminated with matched load. (e) Gain at port-2, port-1 terminated with matched load. (f) Gain with simultaneous excitation.

using Agilent's vector network analyser (VNA model no: N5247A), and the setup along with simulated and measured results is shown in Figure 4(a). For Tx (port-1), it can be observed that the simulated impedance bandwidth (BW), $|S_{11}| \leq -10$ dB, ranges from 5.62 to 5.84 GHz, and the measured values obtained are 5.71-5.88 GHz. Similarly, for Rx (port-2), the simulated BW lies from 5.62 to 5.84 GHz, while the measurements yield 5.73-5.88 GHz. The measured results are in good agreement with the simulated results, while the minor deviations can be attributed to the connector losses and fabrication imperfections. Now, for in-band full-duplex operation, an overlapping frequency band of Tx and Rx antennas is considered. Thus, it can be inferred that the proposed STRA operates in full-duplex mode for a frequency band ranging from 5.73 to 5.88 GHz. The interport isolation values can be obtained from transmission coefficients, $|S_{21}| = |S_{12}|$. The simulated results show isolation ranging from 32.4 to 45.1 dB, and the measured values obtained are better than 35.5 dB to a maximum of 46.5 dB in the frequency band of interest. Next, the radiation properties were measured in an anechoic chamber, and the setup as well as the realized gain results for both ports are shown in Figure 4(b). From the measured values of realized gain, it is evident that the duo is radiating with a gain of 5.45 to 6.00 dBi and 5.00 to 6.50 dBi over the operating bandwidth from port-1 and port-2, respectively. Furthermore, the simulated and measured results of the radiation pattern are plotted in the figure. For port-1, the copolarization (Co-Pol.) and cross-polarization (Cr-Pol) results in the E-plane and H-plane are shown in Figures 5(a) and 5(b), respectively. In the E-plane ($\varphi = 0^\circ$,xz plane), the Co-Pol levels are 15 dB higher than the Cr-Pol levels for $\theta = 0^\circ$, while the maximum margin is obtained for $\theta = 330^\circ$. In the H-plane ($\varphi = 90^\circ$, yz plane), the Co-Pol levels are 25 dB higher than the Cr-Pol levels for $\theta = 0^\circ$. Similarly, for port-2, in the E-plane ($\varphi = 90^\circ$, yz plane), the Co-Pol levels are 28 dB higher than the Cr-Pol for $\theta = 0^\circ$ (Figure 5(c)). In the H-plane ($\varphi = 0^\circ$, xz plane), the Cr-Pol levels are 27 dB lower than the Co-Pol for $\theta = 0^\circ$ (Figure 5(d)). The resultant radiation patterns in E- and H-planes for each port are shown in Figures 5(e) and 5(f), respectively. Furthermore, for better insight about the operational modes of proposed antenna, the simulated E-field patterns and the gain have been demonstrated in Figure 6 for three possible cases, viz., (1) when port-1 is excited and port-2 is terminated with matched load (half-duplex), (2) when port-2 is excited and port-2 is terminated with matched load (half-duplex), and (3) when both port-1 and port-2 are excited simultaneously (full-duplex).

Table 1: Comparison of previously reported LP IBFD antennas.

Ref.	Iso. technique	Isolation (dB)	BW (MHz)	Res. Freq. (GHz)	Size (λ_0^3)
[3]	RT	>36	220	2.5	0.038
[15]	DF	>75	50	2.5	0.006*
[9]	OSPD	>37	520	2.6	0.060
[13]	DR	>20	120	2.4	0.002
[16]	FC and DGS	>45	94	5.9	0.034
This paper	SD, FC, and DGS	>35	150	5.8	0.014

DF: differential feed; RT: reflective terminal; OSPD: orthogonal spatial phase diversity; DR: decoupling resonator; FC: field confinement; GP: ground perturbations; SD: spatial diversity; DGS: defected ground structure. *Excluding the size of the feed network.

To highlight the features of the proposed antenna, a comparison is drawn in Table 1 for various reported linearly polarized STRA or in-band full-duplex (IBFD) antennas. It can be observed that the antenna reported in [15] not only provides very high isolation but also requires the feeding network externally. This increases the overall footprint of the antenna. Similarly, for the antenna in [9], high isolation is achieved for a broad bandwidth of 520 MHz, but the structure has a nonplanar profile due to the implementation of vertical integration for spatial separation. In [3], a reflective terminal-based cancellation is reported to attain isolation better than 35.9 dB. However, the fixed reflective load possesses limitations in dynamic environment conditions.

A compact antenna is reported in [13] which uses a fence strip via structure as a decoupling resonator and offers 20-30 dB of isolation. In [16], the use of via fence along with DGS offers ITS extremely high isolation levels, but for a narrow bandwidth (covers the V2X and application bands). However, in the proposed antenna, by using a combination of spatial diversity, field confinement, and DGS, better impedance bandwidth is obtained which covers V2X, ITS, and CBRS/LTE B48 bands. Furthermore, in comparison to these works, the proposed antenna offers the following advantages: (1) interport isolation ranging from 35.5 to 46.5 dB over a BW of 150 MHz, (2) a relatively compact, planar, simple, and symmetric geometry with a footprint of 0.43 λ_0^2 (λ_0 is the free-space wavelength at resonance frequency) opens a room for full-duplex MIMO implementations, and (3) no additional hardware is required for the feed network.

4. Conclusion

A simple antenna terminal that can transmit and receive within the same frequency band of 5.73 to 5.88 GHz has been realized. This antenna offers high interport isolation (better than 35.5 dB) for an impedance bandwidth of 150 MHz. The antenna utilizes spatial diversity, field confinement, and surface current cancellation techniques for enhanced isolation levels. In addition, the proposed antenna radiates with high gain (better than 5 dBi to a maximum of 6.5 dBi) over the entire frequency range of operation. The planar structure and relatively simple geometry make the proposed antenna attractive for implementing wireless point-to-point or point-to-multipoint communication, or wireless LAN applications in full-duplex mode. As a further study, the symmetric nature of the proposed antenna can be exploited for a compact 8-element full-duplex MIMO implementation.

Data Availability

The data that support the findings of this study are available from the corresponding author upon reasonable request.

Disclosure

This research was performed as part of the employment of the authors (employer: Director, IIT Roorkee).

Conflicts of Interest

The authors declare that there is no potential conflict of interest.

Acknowledgments

The authors would like to acknowledge the Semi-Conductor Laboratory, Ministry of Electronics and Information Technology, Government of India, for supporting this work.

References

[1] I. P. Roberts, J. G. Andrews, H. B. Jain, and S. Vishwanath, "Millimeter-wave full duplex radios: new challenges and techniques," *IEEE Wireless Communications*, vol. 28, no. 1, pp. 36–43, 2021.

[2] M. Heino, D. Korpi, T. Huusari et al., "Recent advances in antenna design and interference cancellation algorithms for in-band full duplex relays," *IEEE Communications Magazine*, vol. 53, no. 5, pp. 91–101, 2015.

[3] X. Wang, W. Che, W. Yang, W. Feng, and L. Gu, "Self-interference cancellation antenna using auxiliary port reflection for full-duplex application," *IEEE Antennas and Wireless Propagation Letters*, vol. 16, pp. 2873–2876, 2017.

[4] H. Nawaz and I. Tekin, "Double-differential-fed, dual-polarized patch antenna with 90 dB interport RF isolation for a 2.4 GHz in-band full-duplex transceiver," *IEEE Antennas and Wireless Propagation Letters*, vol. 17, no. 2, pp. 287–290, 2018.

[5] D. L. Wu, W. J. Zhu, K. Y. Yang, L. H. Ye, and J. F. Li, "Wideband dual-polarized antenna with high isolation for full-

duplex application," *Microwave and Optical Technology Letters*, vol. 64, no. 9, pp. 1649–1656, 2022.

[6] H. Nawaz and I. Tekin, "Dual port single patch antenna with high interport isolation for 2.4 GHz isn-band full duplex wireless applications," *Microwave and Optical Technology Letters*, vol. 58, no. 7, pp. 1756–1759, 2016.

[7] H. Nawaz, M. Basit, and F. Shaukat, "Dual polarized, slot coupled monostatic antenna wsith high isolation for 2.4 GHz full duplex applications," *Microwave and Optical Technology Letters*, vol. 62, pp. 1291–1298, 2020.

[8] K. Kumari, R. Jaiswal, and K. V. Srivastava, "Anin-band full-duplexantenna fordual-bandapplication," *Microwave and Optical Technology Letters*, vol. 64, no. 1, pp. 130–136, 2022.

[9] L. Sun, Y. Li, Z. Zhang, and Z. Feng, "Compact co-horizontally polarized full-duplex antenna with omnidirectional patterns," *IEEE Antennas and Wireless Propagation Letters*, vol. 18, no. 6, pp. 1154–1158, 2019.

[10] A. H. Hussein, H. H. Abdullah, M. A. Attia, and A. M. Abada, "S-band compact microstrip full-duplex Tx/Rx patch antenna with high isolation," *IEEE Antennas and Wireless Propagation Letters*, vol. 18, no. 10, pp. 2090–2094, 2019.

[11] A. N. Nguyen, V. Hoang le, N. Nguyen-Trong et al., "Dual-polarized slot antenna for full-duplex systems with high isolation," *IEEE Transactions on Antennas and Propagation*, vol. 69, no. 11, pp. 7119–7124, 2021.

[12] S. X. Ta, N. Nguyen-Trong, V. C. Nguyen, K. K. Nguyen, and C. Dao-Ngoc, "Broadband dual-polarized antenna using metasurface for full-duplex applications," *IEEE Antennas and Wireless Propagation Letters*, vol. 20, no. 2, pp. 254–258, 2021.

[13] Y. He and Y. Li, "Compact co-linearly polarized microstrip antenna with fence-strip resonator loading for in-band full-duplex systems," *IEEE Transactions on Antennas and Propagation*, vol. 69, no. 11, pp. 7125–7133, 2021.

[14] C. A. Balanis, *Antenna Theory: Analysis and Design*, John Wiley, 2005.

[15] G. Chaudhary, J. Jeong, Y. Jeong, and W. Ham, "Microstrip antenna with high self-interference cancellation using phase reconfigurable feeding network for in-band full duplex communication," *Microwave and Optical Technology Letters*, vol. 62, no. 2, pp. 919–925, 2020.

[16] J. C. Dash and D. Sarkar, "A Colinearly polarized full-duplex antenna with extremely high Tx–Rx isolation," *IEEE Antennas and Wireless Propagation Letters*, vol. 21, no. 12, pp. 2387–2391, 2022.